The effect of detachment and attachment to a kink motion in the asymmetric simple exclusion process

2006 J. Phys. A: Math. Gen. 39 15073

(http://iopscience.iop.org/0305-4470/39/49/002)

INSTITUTE OF PHYSICS PUBLISHING JOURNAL OF PHYSICS A: MATHEMATICAL AND GENERAL

J. Phys. A: Math. Gen. **39** (2006) 15073–15082 doi:10.1088/0305-4470/39/49/002

The effect of detachment and attachment to a kink motion in the asymmetric simple exclusion process

Tetsuya Mitsudo and Hisao Hayakawa[1]

Department of Physics, Yoshida-South campus, Kyoto University, Sakyo-ku, Kyoto, 606-8501 Japan

E-mail: mitsudo@yukawa.kyoto-u.ac.jp and hisao@yukawa.kyoto-u.ac.jp

Received 12 June 2006, in final form 30 October 2006
Published 21 November 2006
Online at stacks.iop.org/JPhysA/39/15073

Abstract

We study the dynamics of a kink in a one-lane asymmetric simple exclusion process with detachment and attachment of particles at arbitrary sites. For a system with one site of detachment and attachment we find that the kink is trapped by the site, and the probability distribution of the kink position is described by the overdumped Fokker–Planck equation with a V-shaped potential. When the detachment and attachment take place at every site, we confirm that the kink motion is equivalent to the diffusion in a harmonic potential. We compare our results with the Monte Carlo simulation, and check the quantitative validity of our theoretical prediction of the potential form.

PACS numbers: 02.50.−r, 05.40.−a

1. Introduction

An asymmetric simple exclusion process (ASEP) is a stochastic process on a one-dimensional lattice where a particle drifts when the site to visit is empty. Recently much attention has been paid to ASEP [1–3], not only because there exists the exact solution under the open boundary condition [4–7], but also it is applicable to various transportation phenomena. In particular, the uni-directional ASEP which is called a totally asymmetric simple exclusion process (TASEP) has been studied extensively, because (i) TASEP is the simplest ASEP and (ii) TASEP keeps the essence of nonequilibrium transport processes such as the exclusion interaction between particles and the drift of particles. In fact, TASEP may be regarded as a simplified model of traffic flow [8].

ASEP is also a relevant model for the description of biological problems. TASEP is first introduced as a model to explain the process of creation of the messenger RNA [9] in 1968.

[1] Present address: Yukawa Institute for Theoretical Physics, Kitashirakawa-Oiwake-Cho, Kyoto University, Sakyo-ku, Kyoto 606-8502, Japan.

Recently, the model with detachment and attachment on each site in ASEP with open boundary conditions has been introduced in the context of describing the collective motion of molecular motors on the microtubules [10, 11]. TASEP with detachment and attachment on each site under open boundary conditions in the thermodynamical limit is studied by Parmegianni *et al* [12]. Hereafter, we call one-dimensional TASEP with detachment and attachment under open boundary conditions the PFF model named after the authors of [12], Parmegianni, Franosch and Frey. An extended model of the PFF model is used to describe an intra-cellular transport of the single-headed kinesin (KIF1A) motor [13].

In the open boundary ASEP without detachment and attachment, we can draw a phase diagram by the incoming rate and outgoing rate at the boundaries. On the phase boundary between the low-density phase and high-density phase, it is known that the kink between a sparse region and a jammed region obeys the Brownian motion. This kink motion in one-lane ASEP is also studied in terms of the domain wall theory [14–16] and the second-class particle [17–19]. The kink motion in a two-lane TASEP is studied in [20], and the kink motion in the PFF model is studied in [21–24]. It is known that the kink is trapped by a harmonic potential in the PFF model [21, 22], which is derived by the theoretical argument of continuous equations in the limit of zero lattice spacing.

The effect of detachment of particles at a site in the centre of the system has been studied in [25]. Evans *et al* [26] studied a system with several sites of detachment and attachment and found the exact solution when the both detachment rate and attachment rate are much larger than the drift rate by keeping the constant ratio of detachment rate to attachment rate. In their case, however, the kink is no longer stable.

In this paper, we find that the attractive potential to the kink is a linear function of distance from the site of detachment and attachment in TASEP. When we generalize the model to TASEP with many sites of detachment and attachment, we confirm that the kink feels the linear combination of the linear potentials for the one site of detachment and attachment. It is noted that our model discussed in this paper includes TASEP and PFF model, which has not been discussed by anyone.

The paper is organized as follows. In the next section, we first introduce the model with detachment and attachment at one site. We present a theory of a kink motion in TASEP with detachment and attachment at one site, and extend our analysis to the kink motion in TASEP with detachment and attachment at many sites. In section 3, we compare our analysis with the Monte Carlo simulation and confirm the quantitative agreement between the theory and the simulation. Finally, we give a discussion and conclude this paper in section 4.

2. The kink motion

2.1. TASEP with one site of detachment and attachment

Let us explain TASEP with detachment and attachment of particles at one site under open boundary conditions. TASEP is defined on a one-dimensional lattice of L sites. Each particle hops forward when the front site is empty. Here we choose right as the drift direction of particles. The open boundary condition is specified by the attachment rate of particle α at the left end of the system and the detachment rate of particle β at the right end. Here, the particle is also detached by the rate w_d and attached by the rate w_a at the site x_0. TASEP with detachment at one site has first been introduced in [25]. In their analysis, they divide the system into two systems of TASEP by the site x_0 which is fixed to the centre of the system, and introduce the effective hopping rate to connect the two systems. However, their analysis cannot explain the kink motion because the kink in TASEP moves under the reflective boundary condition

of a virtual boundary in a subsystem and the kink Cannot cross through the virtual boundary between two subsystems. Thus we need another method to explain the effect of detachment and attachment to the kink motion.

The Brownian motion of the kink is characterized by the two parameters: the drift velocity V_T and the diffusion constant D_T. In the case of TASEP, V_T and D_T are respectively written as [19]

$$V_T = 1 - \lambda_\ell - \lambda_r \qquad \text{and} \qquad D_T = \frac{\lambda_\ell(1-\lambda_\ell) + \lambda_r(1-\lambda_r)}{2(\lambda_r - \lambda_\ell)}, \tag{1}$$

where λ_ℓ and λ_r are the density in the left and in the right, respectively. Thus once λ_ℓ and λ_r which satisfy $\lambda_\ell < \lambda_r$ are known, the motion of the kink is determined.

It is known that the Brownian motion in a potential $U(x)$ is written by the Langevin equation

$$\frac{\mathrm{d}x}{\mathrm{d}t} = -\frac{\partial U(x)}{\partial x} + \zeta(t), \tag{2}$$

where $\zeta(t)$ is the random force which satisfies

$$\langle \zeta(t) \rangle = 0 \qquad \text{and} \qquad \langle \zeta(t)\zeta(0) \rangle = 2D\delta(t), \tag{3}$$

where $\delta(t)$ is Dirac's delta function. The corresponding Fokker–Planck equation to equation (2) is

$$\frac{\partial P(x,t)}{\partial t} = \frac{\partial}{\partial x}\left(\frac{\partial U(x)}{\partial x} + D\frac{\partial}{\partial x}\right) P(x,t), \tag{4}$$

where $P(x,t)$ is the probability distribution of the Brownian particle at position x at time t. Equation (4) has the steady solution $P_{st}(x)$

$$P_{st}(x) = C \exp\left[-\frac{U(x)}{D}\right], \tag{5}$$

where C is the normalization constant. We expect that this result can be used to describe the steady distribution of the kink in TASEP with detachment and attachment.

For TASEP without detachment and attachment, λ_ℓ and λ_r satisfy

$$\lambda_\ell = \alpha \qquad \text{and} \qquad \lambda_r = 1 - \alpha \tag{6}$$

for $\alpha = \beta < 1/2$. From equation (1), V_T and D_T are respectively given by

$$V_T = 0 \qquad \text{and} \qquad D_T = \frac{\alpha(1-\alpha)}{1-2\alpha}. \tag{7}$$

If there is a site with detachment and attachment, the phase diagram may be modified from that of the original TASEP. However the difference is expected to be small for small rate of detachment and attachment ($w_a \sim w_d \ll 1$). Thus the kink picture may be still valid for $\alpha = \beta \ll 1/2$.

Let us consider the kink motion in TASEP with detachment and attachment at one site. If there is no detachment and attachment of particles, λ_ℓ and λ_r are given by equation (6). However, as a result of detachment and attachment, the density is deviated from equation (6). There are two cases for the deviation of the density: (a) the site with detachment and attachment in the low-density region and (b) the site in the high-density region.

Let us consider the case (a). The change of the density in terms of detachment and attachment can be neglected in the region left of x_0, while the density in the right of x_0 becomes higher (figure 1(*a*)). In fact, when the density around the site with detachment and

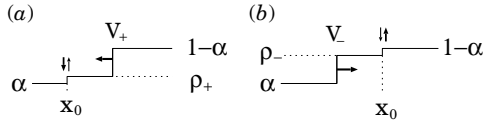

Figure 1. A schematic picture of the kink motion in TASEP with one site of detachment and attachment. Figure (*a*) shows the case when x_0 is in the low-density region, and figure (*b*) shows the case when x_0 is in the high-density region. The line shows the density profile. This density profile is drawn by the ensemble average after the position of the kink is specified.

attachment ρ is low, the attach current $w_a(1-\rho)$ is much larger than the detach current $w_d\rho$ for $w_a \sim w_d$. We introduce ρ_+ as the density in the right of x_0 when x_0 is in the low-density region. Thus λ_ℓ is $\lambda_\ell = \rho_+$ while $\lambda_r = 1-\alpha$ is unaffected. It should be noted that this argument is only valid for the case of $w_d \sim w_a$. If we assume $w_a \ll w_d$, then the density in the right of x_0 is lower than that in the left. In this case, the kink might feel a repulsive force from x_0. However, we do not discuss such cases here. Although one might expect that traffic jams propagate to the left, nobody has found a stable jammed domain in ASEP and no traffic jams propagate.

When x_0 is in the high-density region as in case (b), the density profile is modified as in figure 1(*b*). In this case, the density in the right of x_0 is little changed by detachment and attachment but the density in the left of x_0 is changed by detachment and attachment. For the case the density around the site with detachment and attachment ρ is high, the detach current $w_d\rho$ is much larger than the attach current $w_a(1-\rho)$ for $w_a \sim w_d$. Thus λ_ℓ and λ_r are replaced by $\lambda_\ell = \alpha$ and $\lambda_r = \rho_-$ when x_0 is in the high-density region of the kink.

Now, let us determine the value of ρ_- and ρ_+. Since the exact solution in the steady state of this model is not known, we adopt the decoupling approximation in which the currents J_ℓ in the low-density region and J_r in the high-density region are given by $J_\ell = \lambda_\ell(1-\lambda_\ell)$ and $J_r = \lambda_r(1-\lambda_r)$, respectively. The decoupling approximation is the approximation that the two-point function $\langle\tau_j\tau_{j+1}\rangle$ is given by the product of one point functions $\langle\tau_j\rangle\langle\tau_{j+1}\rangle$, where $\langle\cdots\rangle$ is the average by the probability of finding the system in the state $\{\tau_1,\ldots,\tau_L\}$ with $\tau_j = 0, 1$.

To estimate ρ_+ and ρ_-, we use the current conservation at the position x_0. For the case that x_0 is in the low-density region of the kink, the current from the left of x_0 is $\alpha(1-\alpha)$ and the current to the right of x_0 is $\rho_+(1-\rho_+)$. The detach current from x_0 is $w_d\rho_+$ and the attach current at x_0 is $w_a(1-\rho_+)$. Thus the equation of the current balance at x_0 is given by

$$\alpha(1-\alpha) + w_a(1-\rho_+) = w_d\rho_+ + \rho_+(1-\rho_+). \tag{8}$$

The solution of (8) is simply given by

$$\rho_+ = \frac{1+w_a+w_d-\sqrt{(1+w_a+w_d)^2-4w_a-4\alpha(1-\alpha)}}{2}. \tag{9}$$

Here we use the condition that ρ_+ should be reduced to (6) for $w_a = w_d = 0$. Similarly, the current balance equation of ρ_- is written as

$$\rho_-(1-\rho_-) + w_a(1-\rho_-) = w_d\rho_- + \alpha(1-\alpha), \tag{10}$$

and its solution is given by

$$\rho_- = \frac{1-w_a-w_d+\sqrt{(1-w_a-w_d)^2+4w_a-4\alpha(1-\alpha)}}{2}. \tag{11}$$

From equation (1) with the consideration around figure 1, the drift velocities $V_\pm$ are given by

$$V_+ = \alpha - \rho_+ \qquad \text{and} \qquad V_- = 1 - \alpha - \rho_-. \tag{12}$$

Similarly the diffusion constants $D_\pm$ are given by

$$D_+ = \frac{\alpha(1-\alpha) + \rho_+(1-\rho_+)}{2(1-\alpha-\rho_+)} \qquad \text{and} \qquad D_- = \frac{\alpha(1-\alpha) + \rho_-(1-\rho_-)}{2(\rho_- - \alpha)}. \tag{13}$$

Here the quantities with the suffix $+/-$ represent those in the right/left of x_0. Using $\lambda_\ell = \alpha$, $\lambda_r = \rho_-$ for $x < x_0$ and $\lambda_\ell = \rho_+$, $\lambda_r = 1 - \alpha$ for $x > x_0$, the steady solution of the Fokker–Planck equation can be written as

$$P(x) = C' \exp\left[\frac{V_-}{D_-}(x - x_0)\theta(x_0 - x) + \frac{V_+}{D_+}(x - x_0)\theta(x - x_0)\right], \tag{14}$$

where C' is the normalization constant, and $\theta(x) = 1$ for $x > 0$ and $\theta(x) = 0$ otherwise.

For $w = w_a = w_d$, the relations

$$\rho_- = 1 - \rho_+, \qquad |V_+| = |V_-| \qquad \text{and} \qquad D_+ = D_- \tag{15}$$

are satisfied. Thus the solution (14) becomes

$$P(x) = C' \, \mathrm{e}^{-\frac{V}{D}|x - x_0|}, \tag{16}$$

where $V = |V_-| = |V_+|$ and $D = D_+ = D_-$. From the comparison of equation (5) with equation (16), the potential energy $U(x)$ is given by

$$U(x) = V|x - x_0|. \tag{17}$$

This is one of the main results in this paper. The validity of our theory will be confirmed by the Monte Carlo simulation in section 3.

2.2. TASEP with many sites of detachment and attachment

Here we generalize the model in the previous subsection to a model with many sites of detachment and attachment. To ensure the domain wall picture, we assume that $w \doteq w_a = w_d$ are small and the relations equation (15) are satisfied. Substituting the expansion ρ_+ in terms of w

$$\rho_+ \simeq \alpha + w + \cdots \tag{18}$$

into equation (12), we obtain

$$V = w. \tag{19}$$

In this linear regime, we can obtain the probability function of the kink in TASEP with many sites of detachment and attachment.

Let us consider the system with N sites of detachment and attachment. Here we see that the system is divided into $N + 1$ segments in which each segment is bounded by the sites with detachment and attachment or the boundaries.

When the kink is located in the jth segment, the number of sites with detachment and attachment in the left of the kink is $j - 1$. For each site of detachment and attachment, the current should be conserved. The density increases by w in the low-density region as in

equation (18) in each segment. Thus the density λ_ℓ in the jth segment becomes $\lambda_\ell = \alpha + w(j-1)$. On the other hand, the number of sites with detachment and attachment in the right of the kink is $N - j + 1$. Then the density λ_r in the jth segment is $\lambda_r = 1 - \alpha - w(N - j + 1)$. Therefore, the drift velocity V_j and the diffusion constant D_j in the segment j are respectively given by

$$V_j = w\{N - 2(j-1)\}, \tag{20}$$

and

$$D_j = \frac{2\alpha(1-\alpha) + (1-2\alpha)wN + w^2((N-j)^2 + j^2)}{2(1-2\alpha - wN)}. \tag{21}$$

We can eliminate j-dependence in equation (21) by neglecting the term proportional to w^2. Thus the diffusion coefficient is reduced to

$$D = \frac{2\alpha(1-\alpha) + (1-2\alpha)wN}{2(1-2\alpha - wN)}, \tag{22}$$

which is independent of j. From equation (5), the kink probability distribution $P_j(x)$ in the segment j is given by

$$P_j(x) = C_j \exp\left[-\frac{2w(N-2(j-1))(1-2\alpha - wN)}{2\alpha(1-\alpha) + (1-2\alpha)wN}(x - x_j)\right], \tag{23}$$

where C_j is a constant determined from the normalization and the compatibility relation

$$P_j(x_j) = P_{j+1}(x_j). \tag{24}$$

Thus we obtain the formula equation (23) applicable to TASEP with any number of sites with detachment and attachment. It should be noted that the denominator in the exponential function in equation (23) contains wN. This is because we simply substitute D in equation (22) into equation (5). It may be controversial to contain wN in the denominator in the systematic approximation, but this expression gives us the accurate result as will be shown later.

This method is also applicable to the PFF model [12] where the number of detachment and attachment sites N is $N = L$ and the position of the site of detachment and attachment x_j is $x_j = j$. Thus the distribution (23) is reduced to $P_j(j) = C_j$. We write $P_j = P_j(j)$ for the simplification. The compatibility relation (24) becomes

$$C_j = C_{j-1} \exp\left[\frac{w(L - 2(j-1))}{D}\right], \tag{25}$$

and this recursion relation gives

$$C_j = C_1 \exp\left[\frac{w}{D}\sum_{m=1}^{j-1}(L - 2m)\right]. \tag{26}$$

Thus the distribution function becomes

$$P_j = C_1 \exp\left[\frac{w}{D}\left\{-\left(j - \frac{L+1}{2}\right)^2 + \frac{(L-1)^2}{4}\right\}\right]. \tag{27}$$

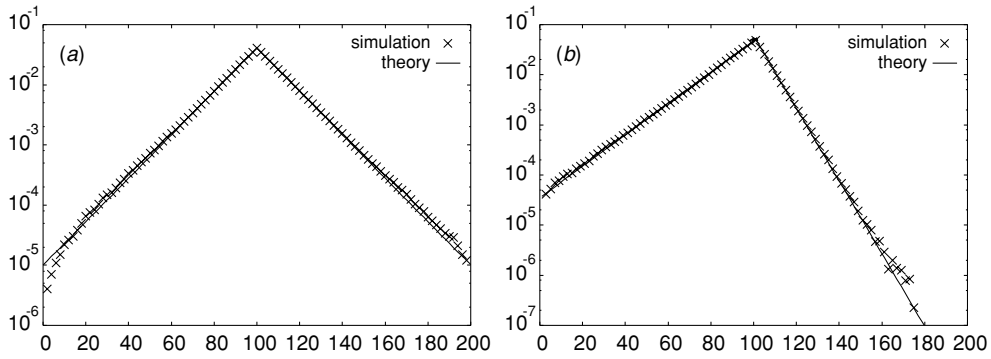

Figure 2. Comparison of the distribution of the kink position between the simulation (×) and the solution of the Fokker–Planck equation (solid line).The horizontal axis is the kink position and the vertical axis is the distribution function of the kink position in the steady state plotted in the semi-log scale. The parameters used are $\alpha = \beta = 0.1$ and $w_a = w_d = 0.01$ for (a), and $\alpha = \beta = 0.1$, $w_a = 0.02$ and $w_d = 0.01$ for (b). We set the system length $L = 200$ and the position of detachment and attachment occurs at $x_0 = 100$.

This result can be also derived by the superposition of the potential. The harmonic potential is realized by the superposition of the potential (17) as

$$U_{\mathrm{PFF}}(j) = \sum_{x_0=1}^{L} w|j - x_0| \simeq w\left(j - \frac{L+1}{2}\right)^2 + \cdots. \tag{28}$$

Thus the distribution of the kink position is given by

$$P_{\mathrm{PFF}}(j) = C'' \exp\left[-\frac{w}{D}\left(j - \frac{L+1}{2}\right)^2\right], \tag{29}$$

where D is given by equation (22), and the probability distribution function of the kink position (29) is identical to equation (27).

3. Simulations

Now let us check the quantitative accuracy of our theoretical argument. We compare our analysis with the results of the Monte Carlo simulations. The simulation is carried out by the random update scheme [3, 27] which is realized by choosing a bond between two neighbouring sites at random in the time interval dt and moving the particle to the front site.

We use the motion of the second-class particle which is a tracer particle to detect the kink position [17–19]. If we write 0 for a hole (empty site), 1 for a particle and 2 for the second class particle, the second class particle moves as $(2, 0) \to (0, 2)$ and $(1, 2) \to (2, 1)$. The hole is moved to the left of the second class particle, and the particle is moved to the right of the second class particle. Thus the second class particle is positioned between the low-density region and the high-density region. Thus the second class particle can detect the kink position. We compare the probability function of the kink position obtained by the simulation with the distribution function (14).

As shown in figure 2, we obtain good agreement between the simulation and the theoretical results in equation (14). We plot the results of our simulation by × and the solution of the Fokker–Planck equation by the solid line. The horizontal axis is the kink position and the

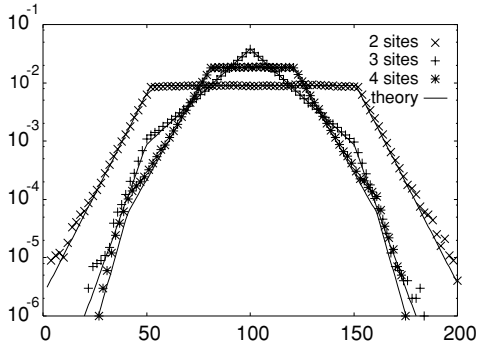

Figure 3. Comparison of the probability distribution of the kink position between the simulation and the solution of the Fokker–Planck equation (solid lines) in equation (23) for the case which has 2(×), 3(+) and 4(∗) sites of detachment and attachment. The horizontal axis is the kink position and the vertical axis is the probability function of the kink position in the steady state plotted in the semi-log scale. The parameters used are $\alpha = \beta = 0.1$ and $w = 0.01$, and the positions of sites with detachment and attachment are $x_1 = 50, x_2 = 150$ for $N = 2, x_i = 50i, (i = 1, 2, 3)$ for $N = 3$ and $x_i = 40i, (i = 1, 2, 3, 4)$. We set the system length $L = 200$.

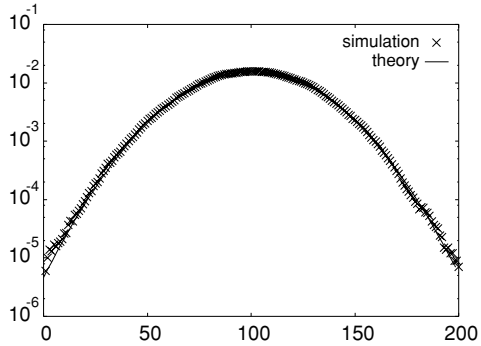

Figure 4. Comparison of the probability distribution of the kink position between the simulation (×) and the solution of (equation (23)) the Fokker–Planck equation (solid line) of PFF model. The horizontal axis is the kink position and the vertical axis is the distribution function of the kink position in the steady state plotted in the semi-log scale. The parameters used are $\alpha = \beta = 0.1$, $w = 0.0001$ and $L = 200$.

vertical axis is the probability distribution function of the kink position in the steady state. In figure 2(a), the parameter is set to be $w_a = w_d$ and the distribution function is symmetric around $x = x_0$. In figure 2(b), the parameter is set to be $w_a \neq w_d$ and the distribution function is asymmetric around $x = x_0$. In both cases, the boundary parameters are set to be $\alpha = \beta = 0.1$ and the system length L is $L = 200$. In figure 3, we compare the theoretical results with the results of our simulation in cases of 2, 3 and 4 sites with detachment and attachment. The parameters used in this case are $\alpha = \beta = 0.1$ and $w = 0.01$, the position of sites with detachment and attachment are $x_1 = 50, x_2 = 150$ for $N = 2, x_i = 50i, (i = 1, 2, 3)$ for $N = 3$ and $x_i = 40i, (i = 1, 2, 3, 4)$. The results of our simulation are plotted by $\times$ for $N = 2, +$ for $N = 3$ and $*$ for $N = 4$, and the theoretical results are plotted in the solid lines. In figure 4, we compare the theoretical results with the simulation results in the PFF model. The parameters at the boundaries are $\alpha = \beta = 0.1$ and $w = 0.0001$. The results of

our simulation give quite good agreement with the theoretical prediction in equation (23) in all cases.

4. Discussion and conclusion

Now let us discuss our results. Although our analysis is not rigorous, the accuracy of our result has been verified by the numerical simulations. Thus we need to explain why we obtained good results. In this paper, we adopt two approximations: the domain wall theory and the decoupling approximation in each domain.

We use domain wall theory (DWT) in determining D and V. It is not proven whether we may adopt the rigorous result in ASEP [17–19] here. We expect that DWT can be used for small enough α and w.

We use decoupling approximation in section 2 to determine $\rho_{\pm}$. We cannot measure the correlation of the low/high region directly in the kink diffusion, however we can measure the correlation in the low/high density region with the kink position fixed. In the low/high density region, a flat density profile is realized, and the decoupling approximation gives a good approximation.

We derived the distribution function of the kink in the PFF model, which is also derived in [21]. The prefactor $\frac{w}{D}$ of $\left(j - \frac{L+1}{2}\right)^2$ in equation (29) differs from the result in [21] only by the order of w^2L^2 which is small and is neglected in this paper. This also supports the validity of our results.

We have demonstrated that the kink motion in TASEP with detachment and attachment can be described by the Brownian motion under the influence of the attractive force from the sites where detachment and attachment take place. We have obtained the attractive potential to the kink and the diffusion constant of the kink. We demonstrate that the superposition of the potentials of our model gives good results for any number of sites with detachment and attachment when the rates of detachment and attachment are small. We compare our result with the simulation and have confirmed that our theoretical prediction of our theory gives quantitatively correct results. We also explain why the kink in the PFF model feels a harmonic potential [21, 22], and succeed the quantitative estimation of the potential.

Acknowledgments

We would like to thank S Takesue for fruitful discussion. This work is partially supported by the Grant-in-Aid for Ministry of Education, Science and Technology(MEXT), Japan (grant No. 18540371), the Grant-in-Aid for the 21st century COE 'Center for Diversity and Universality in Physics' from MEXT, Japan, and the Grant-in-Aid of Japan Space Forum.

References

[1] Schütz G M 2001 Exact solvable models for many-body systems far from equilibrium *Phase Transitions and Critical Phenomena* Vol 19 ed C Domb and J L Lebowitz (London: Academic)
[2] Schmittmann B and Zia R K P 1994 Statistical mechanics of driven diffusive systems *Phase Transitions and Critical Phenomena* Vol 17 ed C Domb and J L Lebowitz (London: Academic)
[3] Spohn H 1991 *Large Scale Dynamics of Interacting Particles* (New York: Springer)
[4] Derrida B, Evans M R, Hakim V and Pasquier V 2003 *J. Phys. A: Math. Gen.* **26** 1493
[5] Schütz G M and Domany E 1993 *J. Stat. Phys.* **72** 277
[6] Sasamoto T 1999 *J. Phys. A: Math. Gen.* **32** 7109
[7] Uchiyama M, Sasamoto S and Wadati M 2004 *J. Phys. A: Math. Gen.* **37** 4958
[8] Helbing D 2001 *Rev. Mod. Phys.* **73** 1067

[9] MacDonald C T, Gibbs J H and Pipkin A C 1968 *Biopolimers* **6** 1
[10] Lipowsky R, Klumpp S and Nieuwenhuizen Th M 2001 *Phys. Rev. Lett.* **87** 108101
[11] Lipowsky R and Klumpp S 2003 *J. Stat. Phys.* **113** 233
[12] Parmegiani A, Franosch T and Frey E 2003 *Phys. Rev. Lett.* **90** 086601
[13] Nishinari K, Okada Y, Schadschneider A and Chowdhury D 2005 *Phys. Rev. Lett.* **95** 118101
[14] Kolomeisky A B, Schütz G M, Kolomeisky E B and Straley J P 1998 *J. Phys. A: Math. Gen.* **31** 6911
[15] Santen L and Appert C 2002 *J. Stat. Phys.* **106** 187
[16] Takesue S, Mitsudo T and Hayakawa H 2003 *Phys. Rev.* E **68** 015103
[17] Ferrari P A, Kipnis C and Saada E 1991 *Ann. Prob.* **19** 226
[18] Ferrari P A 1992 *Prob. Theor. Rel. Fields* **91** 81
[19] Ferrari P A and Fontes L R G 1994 *Prob. Theor. Rel. Fields* **99** 305
[20] Mitsudo T and Hayakawa H 2005 *J. Phys. A: Math. Gen.* **38** 3087
[21] Evans M R, Juhász R and Santen L 2003 *Phys. Rev.* E **68** 026117
[22] Juhász R and Santen L 2004 *J. Phys. A: Math. Gen.* **37** 3933
[23] Mukherji S and Bhattacharjee S M 2005 *J. Phys. A: Math. Gen.* **38** L285
[24] Popkov V, Rákos A, Willmann R D, Kolomeisky A B and Schütz G M 2003 *Phys. Rev.* E **67** 066117
[25] Mirin N and Kolomeisky A B 2003 *J. Stat. Phys.* **110** 811
Mirin N and Kolomeisky A B 2003 *J. Stat. Phys.* **69** 667
[26] Evans M R, Hanney T and Kafri Y 2004 *Phys. Rev.* E **70** 066124
[27] Rajewsky N, Santen L, Schadschneider A and Schreckenberg M 1998 *J. Stat. Phys.* **92** 151